



저작자표시-비영리-변경금지 2.0 대한민국

이용자는 아래의 조건을 따르는 경우에 한하여 자유롭게

- 이 저작물을 복제, 배포, 전송, 전시, 공연 및 방송할 수 있습니다.

다음과 같은 조건을 따라야 합니다:



저작자표시. 귀하는 원저작자를 표시하여야 합니다.



비영리. 귀하는 이 저작물을 영리 목적으로 이용할 수 없습니다.



변경금지. 귀하는 이 저작물을 개작, 변형 또는 가공할 수 없습니다.

- 귀하는, 이 저작물의 재이용이나 배포의 경우, 이 저작물에 적용된 이용허락조건을 명확하게 나타내어야 합니다.
- 저작권자로부터 별도의 허가를 받으면 이러한 조건들은 적용되지 않습니다.

저작권법에 따른 이용자의 권리는 위의 내용에 의하여 영향을 받지 않습니다.

이것은 [이용허락규약\(Legal Code\)](#)을 이해하기 쉽게 요약한 것입니다.

[Disclaimer](#)

Inhibition of excessive autophagy
ameliorates mesenteric artery
dysfunction in angiotensin II-induced
hypertensive mice

Youngin Kwon

Department of Medical Science
The Graduate School, Yonsei University

Inhibition of excessive autophagy
ameliorates mesenteric artery
dysfunction in angiotensin II-induced
hypertensive mice

Youngin Kwon

Department of Medical Science
The Graduate School, Yonsei University

Inhibition of excessive autophagy
ameliorates mesenteric artery
dysfunction in angiotensin II-induced
hypertensive mice

Directed by Professor Young-Ho Lee

The Doctoral Dissertation
submitted to the Department of Medical Science,
the Graduate School of Yonsei University
in partial fulfillment of the requirements for the degree
of Doctor of Philosophy

Youngin Kwon

December 2020

This certifies that the Doctoral
Dissertation of Youngin Kwon is
approved.

Thesis Supervisor : Young-Ho Lee

Thesis Committee Member#1 : Myung-Shik Lee

Thesis Committee Member#2 : Duck Sun Ahn

Thesis Committee Member#3 : Young Won Yoon

Thesis Committee Member#4 : Soo-Kyoung Choi

The Graduate School
Yonsei University

December 2020

ACKNOWLEDGEMENTS

First of all, I am deeply grateful to my professor, Young-Ho Lee, for his guidance and support in completing doctoral dissertation. Without his guidance, this dissertation would not have been made possible.

I would like to appreciate the doctoral committee members, Myung-Shik Lee, Duck Sun Ahn, Young Won Yoon and Soo-Kyoung Choi for their expert advice. Professor Duck Sun Ahn always showed his keen interest on my study and also gave comments and advice to develop into the better study. I would like to express my special thanks of gratitude to Dr. Soo-Kyoung Choi for her guidance and encouragement in carrying out my study.

Also, I would like to thank my lab members. Seonhee always have helped me and be my friend. Chaeun, although we were together for a short time, I would like to thank her for helping me. In addition, I appreciate all professors and members of department of physiology.

Lastly, I would like to thank my parents and brother who be there for me and encourage me. I express deep gratitude to Taeyeon who always support me. It is honor to have these people beside me.

TABLE OF CONTENTS

ABSTRACT	1
I. INTRODUCTION	3
II. MATERIALS AND METHODS	6
1. Cell culture	6
2. Animal models and tissue preparation	6
3. Blood pressure measurements	7
4. Functional studies	7
5. Western blot analysis	8
6. Immunofluorescence staining	9
7. Acridine orange staining	9
8. RNA preparation and real-time PCR	10
9. Determination of nitric oxide	10
10. Statistical analysis	11
III. RESULTS	
1. Ang II-induced changes on expression levels of autophagic markers in VSMCs	12
2. Effects of autophagy inhibitors on expression levels of autophagic markers in VSMCs	14
3. Effects of autophagy inhibitors on contractile responses in mesenteric arteries	17
4. Effects of autophagy inhibitor on blood pressure	20
5. Effects of autophagy inhibitors on expression levels of autophagic markers in mesenteric arteries and aortas from Ang II-induced hypertensive mice	22

6. Effects of autophagy inhibitors on endothelium-dependent relaxation in mesenteric arteries from Ang II-induced hypertensive mice.....	25
7. Autophagy inhibitor increases nitric oxide production in HUVECs and mesenteric arteries.....	28
IV. DISCUSSION.....	31
V. CONCLUSION.....	36
REFERENCES.....	37
ABSTRACT(IN KOREAN).....	43
PUBLICATION LIST.....	45

LIST OF FIGURES

Figure 1. Effects of Ang II on the expression of autophagic markers in primary VSMCs	13
Figure 2. Effects of autophagy inhibitors on the expression levels of autophagic markers in primary VSMCs	15
Figure 3. Dose-dependent response to chloroquine and 3-methyladenine in mesenteric arteries pre-contracted with U46619	18
Figure 4. Effects of autophagy inhibitor on blood pressure and body weight	21
Figure 5. Effects of autophagy inhibitor on autophagic markers in aortas and mesenteric arteries from Ang II-induced hypertensive mice	23
Figure 6. Effects of autophagy inhibitor on endothelium-dependent relaxation in mesenteric arteries from Ang II-induced hypertensive mice	26
Figure 7. Effects of autophagy inhibitor on nitric oxide production in mesenteric arteries and HUVECs	29

ABSTRACT

Inhibition of excessive autophagy ameliorates mesenteric artery dysfunction in angiotensin II-induced hypertensive mice

Youngin Kwon

*Department of Medical Science
The Graduate School, Yonsei University*

(Directed by Professor Young-Ho Lee)

Autophagy is an intracellular degradation system that disassembles cytoplasmic components through autophagosomes fused with lysosomes. Recently, the involvement of autophagy in cardiovascular diseases, including pulmonary hypertension, atherosclerosis, and myocardial ischemia, has attracted considerable research attention. However, the role of autophagy in hypertension is not well understood. In the present study, we hypothesized that autophagy contributes to the dysfunction of mesenteric arteries in angiotensin II (Ang II)-induced hypertensive mice. Ang II increased beclin1 and LC3 II expression and decreased p62 expression in vascular smooth muscle cells. Chloroquine, an autophagy inhibitor, increased the expression of beclin1, LC3 II, and p62. 3-methyladenine, an autophagy inhibitor, decreased beclin1 and LC3 II expression and increased p62 expression in vascular smooth muscle cells. Chloroquine and 3-methyladenine dose-dependently dilated arteries pre-contracted by U46619. To determine the role of autophagy in hypertension in vivo, we treated Ang II-induced hypertensive mice with

3-methyladenine ($30 \text{ mg} \cdot \text{kg}^{-1} \cdot \text{day}^{-1}$). Treatment with Ang II increased the blood pressure significantly. Co-treatment with Ang II and 3-methyladenine reduced the blood pressure of Ang II-treated mice. Endothelium-dependent relaxation was significantly impaired in Ang II-treated mice, which was recovered by treatment with 3-methyladenine. We measured the fluorescence intensity of DAF-FM diacetate, an indicator of nitric oxide, to detect the production of nitric oxide. The fluorescence intensity of DAF-FM diacetate was reduced in the mesenteric arteries of Ang II-induced hypertensive mice, which was restored by treatment with 3-methyladenine. p-eNOS (S1177) expression decreased in the mesenteric arteries of Ang II-treated mice, which was reversed by treatment with 3-methyladenine. Therefore, autophagy inhibition ameliorates elevated blood pressure in Ang II-induced hypertensive mice, which is associated with improvement in endothelium-dependent relaxation. These results suggest that autophagy inhibition exerts beneficial effects on the dysfunction of mesenteric arteries in hypertension.

Key words : autophagy, hypertension, angiotensin II, mesenteric artery, endothelium-dependent relaxation

Inhibition of excessive autophagy ameliorates mesenteric artery
dysfunction in angiotensin II-induced hypertensive mice

Youngin Kwon

*Department of Medical Science
The Graduate School, Yonsei University*

(Directed by Professor Young-Ho Lee)

I. INTRODUCTION

Essential hypertension is one of the most common chronic diseases that can cause serious public health problems.¹ Hypertension is defined as a lasting increase in systolic blood pressure ≥ 140 mmHg or diastolic pressure ≥ 90 mmHg. There are various contributors to hypertension such as vascular hypertrophy, increased peripheral vascular resistance, and endothelial dysfunction.²

Peripheral resistance is determined by several factors, including vascular reactivity, which is controlled by endothelium-dependent relaxation.³ The vascular endothelium plays an important role in the regulation of vascular tone by releasing vasodilators such as nitric oxide and vasoconstrictor substances. Several studies have suggested that impaired endothelium-dependent vasodilation is associated with the pathogenesis of cardiovascular diseases such as atherosclerosis and systemic and pulmonary hypertension.^{4,5}

Angiotensin II (Ang II) is an octapeptide hormone of the renin-angiotensin system (RAS).⁶ There are two classes of Ang II receptors: Ang II types 1 and 2. Through the Ang II type 1 receptor, Ang II increases blood pressure by causing

vasoconstriction and releasing aldosterone that promotes sodium retention in the collecting duct.^{7,8} Activation of the Ang II type 1 receptor activates both nicotinamide adenine dinucleotide phosphate (NADPH) and nicotinamide adenine dinucleotide (NADH) oxidases, leading to the production of reactive oxygen species.⁹ In addition, Ang II promotes cell hypertrophy, proliferation, migration, and differentiation, which results in the progression of diseases.^{6,10}

Autophagy is an intracellular degradation system that involves the delivery of cytoplasmic constituents to the lysosome. It is essential for cell survival, differentiation, development, and homeostasis. In the process of autophagy, cells form double-membrane vesicles called autophagosomes. Autophagosomes fuse with the lysosome to degrade the materials it contains.¹¹⁻¹³ The process of autophagy involves over 20 core autophagy-related (Atg) proteins in mammals.¹⁴ Beclin1 is a core component of the class III phosphatidylinositide 3-kinase (PI3K) complex, which promotes phagophore nucleation. The class III PI3K complex produces phosphatidylinositol-3-phosphate on the phagophore membrane to recruit Atg proteins involved in autophagosome formation.^{15,16} The ubiquitin-like LC3 is involved in the elongation of the phagophore. LC3 II is a membrane-bound form that is modified through the conjugation of phosphatidylethanolamine to the carboxyl glycine. LC3 II is integrated into the growing phagophore and remains an autophagosome membrane until autolysosomes.^{16,17} The adapter molecule p62/sequestosome 1 has a multi-domain that comprises a ubiquitin-binding domain and an LC3-interacting region. It binds with ubiquitinated cargoes and then delivers them to autophagosomes.^{18,19} Consequently, beclin1, LC3 II, and p62 are predictors of autophagic flux.

Autophagy maintains cellular homeostasis by supplying metabolites and energy to the cells and eliminating damaged organelles by degrading cellular constituents. However, excessive and uncontrolled autophagy may cause cell death and senescence by leading to the depletion of essential molecules and

organelles.^{20,21} Several clinical and experimental studies have suggested that autophagy is involved in atherosclerosis and pulmonary hypertension.²²⁻²⁴ The levels of autophagy markers increase in the lung tissue of patients with pulmonary hypertension. Consistent with studies on humans, pulmonary hypertension in monocrotaline rat model has been found to be associated with increased autophagy.^{22,25} The role of autophagy in atherosclerosis is controversial. Targeted deletion of Atg7 in mice accelerates aneurysm formation and rupture, thus demonstrating that autophagy has protective effects on atherosclerosis.²⁶ In contrast, autophagy in atherosclerosis leads to the formation and accumulation of ceroids induced by lipid peroxidation.^{24,27} Moreover, *in vivo* and *in vitro* studies have shown that Ang II contributes toward inducing autophagy in cardiomyocytes, cardiac fibroblasts, podocytes, endothelial cells, and vascular smooth muscle cells.²⁸⁻³³ The first evidence is that the Ang II type 1 receptor mediates Ang II-induced autophagy in cardiomyocytes.²⁸ Induction of autophagy by Ang II contributes to hypertrophy in vascular smooth muscle cells and cardiomyocytes.^{33,34} In podocytes, Ang II promotes autophagy through oxidative stress.³⁰ Moreover, autophagy inhibitor administrations or LC3B gene silencing reduces elevated arterial pressure in spontaneously hypertensive rats.³⁵ However, the involvement of autophagy in vascular dysfunction resulting from hypertension has not been characterized.

In the present study, we hypothesized that excessive autophagy might be involved in the progression of Ang II-induced hypertension. Moreover, inhibition of autophagy may ameliorate vascular dysfunction in Ang II-induced hypertension.

II. MATERIALS AND METHODS

All experiments were performed according to the Guide for the Care and Use of Laboratory Animals published by US National Institutes of Health (NIH publication no. 85–23, 2011) and were approved by the Ethics Committee and the Institutional Animal Care and Use Committee of Yonsei University, College of Medicine (Approval number: 2019-0308).

Cell culture

Aortic vascular smooth muscle cells (VSMCs) were obtained from 8-week-old male Sprague-Dawley rats. The rats were euthanized with oxygen and 5% inhalational isoflurane using isoflurane vaporizer (Vapor 19.3; Dräger, Lubeck, Germany), and then euthanized by cardiac excision. The thoracic aorta was removed and placed in Dulbecco's modified Eagle medium (DMEM; Gibco, Life Technologies, Carlsbad, CA, USA). After removing the connective tissues, the aorta was transferred to an enzyme dissociation mixture containing DMEM with 1 mg/mL collagenase (Worthington, Lakewood, NJ, USA) and 0.5 mg/mL elastase (Worthington) with subsequent removal of adventitia. The suspension was centrifuged, and the pellet was resuspended in DMEM supplemented with 10% FBS and 1% penicillin/streptomycin solution. Human umbilical vein endothelial cells (HUVECs) were obtained from the American Type Culture Collection (ATCC, Rockville, MD, USA) and cultured in vascular cell basal medium (ATCC) supplemented with Endothelial Cell Growth Kit-BBE (ATCC). Cultured cells from passages 2–9 were used.

Animal models and tissue preparation

Eight-week-old male C57BL/6 mice were anesthetized with oxygen and 1.5–2.5% inhalational isoflurane throughout surgery. We used surgical scissors to create an approximately 1 cm incision in the mid-scapular region to implant

an osmotic mini-pump (model 2004; Alzet, Cupertino, CA, USA). Mini-pumps were loaded with either Ang II (Merck, Burlington, MA, USA) dissolved in saline or saline alone. Ang II was infused at $1000 \text{ ng}\cdot\text{kg}^{-1}\cdot\text{min}^{-1}$ for 4 weeks. The mice were divided into four groups: (i) vehicle-treated mice; (ii) vehicle-treated mice that received an autophagy inhibitor (3-methyladenine, $30 \text{ mg}\cdot\text{kg}^{-1}\cdot\text{day}^{-1}$); (iii) Ang II-treated mice; and (iv) Ang II-treated mice that received an autophagy inhibitor (3-methyladenine). After 4 weeks of Ang II infusion, the mice were sacrificed through respiratory anesthesia using 1.5–2.5% isoflurane, and then euthanized by cardiac excision. The arteries were immediately excised and placed in chilled Krebs-Henseleit (K-H) solution [composed of (in mM) NaCl, 119; KCl, 4.6; CaCl_2 , 2.5; MgSO_4 , 1.2; KH_2PO_4 , 1.2; NaHCO_3 , 25; glucose, 11.1 (Sigma-Aldrich, St.Louis, MO, USA).] The adipose and connective tissues were removed under an optical microscope (model SZ-40, Olympus, Japan).

Blood pressure measurements

Systolic blood pressure was measured in 7- to 12-week-old mice using the tail-cuff method with a photoplethysmography blood pressure monitoring system (BP-2000, Visitech Systems, Apex, NC, USA). Before the implantation of a mini-pump, the mice were trained using the blood pressure monitoring device for 1 week. On each measurement day, 10 readings were obtained from each mouse.

Functional studies

The segment of the second branch mesenteric artery (130–200 μm in inner diameter) was cannulated on glass micropipettes in a Pressure Servo System PS/200 (Living Systems Instrumentation, Burlington, VT, USA). The heated K-H solution was superfused to the vessel chamber continuously to maintain a temperature of $37 \text{ }^\circ\text{C}$. During the 30-min equilibration period, the pressure was

maintained at 40 mmHg using pressure-servo control perfusion systems. The lumen diameter was measured using the Soft Edge Acquisition Subsystem (IonOptix, Milton, MA, USA). Isometric tension was recorded on the mesenteric arteries in a wire myograph (Danish Myo Technology, Aarhus, Denmark). The mesenteric arteries were set to a basal force of 2 mN. The data were recorded and analyzed using LabChart7 (ADInstruments, Dunedin, New Zealand). All mesenteric arteries were initially contracted with high K^+ solution (70 mM KCl in K-H solution). To further contract the mesenteric arteries, we used phenylephrine (10 μ M; α 1-adrenergic receptor agonist; Sigma-Aldrich), U46619 (100 nM; thromboxane A2 receptor agonist; Cayman Chemicals, Ann Arbor, MI, USA), and high K^+ solution. Chloroquine diphosphate and 3-methyladenine were purchased from Sigma-Aldrich and Cayman Chemicals, respectively. The arteries were pre-contracted with phenylephrine and endothelium-dependent relaxation was measured in response to cumulative doses of acetylcholine (10^{-9} – 10^{-5} M, Sigma-Aldrich). The endothelium-denuded arteries were confirmed by the absence of response to acetylcholine. A nitric oxide donor, sodium nitroprusside dihydrate (disodium pentacyanonitrosylferrate(2-)dihydrate, Sigma-Aldrich) was used as a vasodilator.

Western blot analysis

Western blotting was performed in the aortas, mesenteric arteries, VSMCs, and HUVECs. All the samples were homogenized in ice-cold RIPA buffer (radioimmunoprecipitation assay buffer; Sigma-Aldrich) with complete protease and phosphatase inhibitor cocktail (Thermo Scientific, Waltham, MA, USA). After lysis, tissue debris was removed by centrifugation, and cleared protein lysates were used. The samples were loaded in 8–15% SDS-PAGE gels. The separated proteins were transferred to nitrocellulose membranes. The membranes were incubated with primary antibodies against the following

antigens: Beclin1 (1:4000, Cell Signaling, Boston, MA, USA), LC3 A/B (1:4000, Cell Signaling), p62 (1:4000, Abcam, Cambridge, MA, USA), p-eNOS (S1177, 1:1000, Invitrogen, Carlsbad, CA, USA), total eNOS (1:1000, Invitrogen), and β -actin (1:5000, Abcam). HRP-conjugated anti-rabbit and anti-mouse (Merck) secondary antibodies were used.

Immunofluorescence staining

Beclin1 expression in the mesenteric arteries was measured by using immunofluorescence staining. The vessels were cleaned of connective tissue and cut into 4–5 mm long sections. The cleaned arteries were immediately embedded in OCT and frozen in liquid nitrogen. The frozen sections (5 μ m) were serially collected and blocked with PBS containing 3% bovine serum albumin. After blocking, the arteries were incubated with beclin1 (1:100; Abcam) and smooth muscle actin (1:100; Abcam). Streptavidin-conjugated Alexa Fluor 488 and Alexa Fluor 594 (1:100; Invitrogen) secondary antibodies were used. DAPI was used for nuclear staining (Vector Laboratories, Burlingame, CA, USA). Immunofluorescence images were obtained using a laser scanning confocal microscope (LSM700, Carl Zeiss, Oberkochen, Germany). Immunofluorescence intensity was quantified using Image J (National Institutes of Health, Bethesda, MD, USA).

Acridine orange staining

Acridine orange (Invitrogen) is a lysosomotropic dye used to stain acidic vesicular organelles.³⁶ Acidic organelles such as autolysosomes and lysosomes have an internal pH of 5. Acridine orange enters into lysosomes and becomes protonated.³⁷ Protonated acridine orange aggregates and emits red fluorescence. The VSMCs were subcultured in 12 mm coverslips with poly L-lysine coating. After starvation for 24 h, VSMCs were incubated in a serum-free medium treated with Ang II or co-treated with Ang II and 3-methyladenine for 24 h,

exposed to acridine orange (1 $\mu\text{g}/\text{mL}$) for 15 min, and then washed with PBS. After fixation with 4% paraformaldehyde, VSMCs were examined under a laser scanning confocal microscope (Carl Zeiss) with a 60 \times water immersion objective. The excitation/emission wavelengths for green and red fluorescence were 488/518 nm and 555/573 nm, respectively.

RNA preparation and real-time PCR

Total RNA was isolated from the aortas using an RNA extraction kit (GeneAll Biotechnology Co. Ltd, Seoul, Korea). The isolated RNA (1 μg) was used to synthesize complementary DNA (cDNA) using a cDNA synthesis kit (Takara Bio, Shiga, Japan). Real-time PCR was performed with SYBR Green (Takara) using a Step-One Plus System (Applied Biosystems, Foster City, CA, USA). The following primers were used for the reaction: mouse p62 forward 5'-GTC AAG ATG GAG CCG GAG AA-3'; mouse p62 reverse 5'-CGG GTC GAG CGA GTC CTT-3'; mouse actin forward 5'-AAA TCG TGC GTG ACA TCA AAG A-3'; and mouse actin reverse 5'-GCC ATC TCC TGC TCG AAG TCT-3'. The reaction conditions were as follows: initial denaturation at 95 $^{\circ}\text{C}$ for 30 s, 40 amplification cycles at 95 $^{\circ}\text{C}$ for 5 s and 60 $^{\circ}\text{C}$ for 30 s. The relative amount of p62 mRNA was calculated by using the $2^{-\Delta\Delta\text{CT}}$ (CT, comparative threshold cycle) method. $\Delta\Delta\text{CT}$ was calculated using the following formula: $\Delta\Delta\text{CT} = (\text{CT}_{\text{p62}} - \text{CT}_{\text{actin}})_{\text{Ang II}} - (\text{CT}_{\text{p62}} - \text{CT}_{\text{actin}})_{\text{vehicle}}$.

Determination of nitric oxide levels

Nitric oxide production in mesenteric arteries was measured as previously described.³⁸ The mesenteric arteries were incubated in DAF-FM diacetate (5 μM ; 4-amino-5-methylamino-2', 7'-difluorofluorescein diacetate; Cayman Chemicals) and acetylcholine (1 μM ; for 30 min at 37 $^{\circ}\text{C}$ in K-H solution). The arteries were washed with the K-H solution and images were acquired using an Olympus BX51 microscope (Olympus). The fluorescent images were analyzed

using Image J software (National Institutes of Health).

Statistical analysis

Results were expressed as mean \pm SEM. Comparisons between groups were performed with Student's *t* tests. Values of $p < 0.05$ were considered significant. The concentration-response curve was fitted to sigmoidal curve with a variable slope using four parameters logistic equation in GraphPad Prism (Version 7, GraphPad software, La Jolla, CA, USA).

III. RESULTS

Ang II-induced changes in the expression of autophagic markers in VSMCs

To evaluate whether Ang II promotes autophagy, we incubated VSMCs with Ang II (10^{-8} – 10^{-6} mol/L) for 24 h (Fig. 1). Ang II dose-dependently increased the expression of beclin1 and LC3 II, whereas Ang II decreased the expression of p62 (Fig. 1B–D). Based on these results, we assumed that Ang II induced autophagic flux in VSMCs.

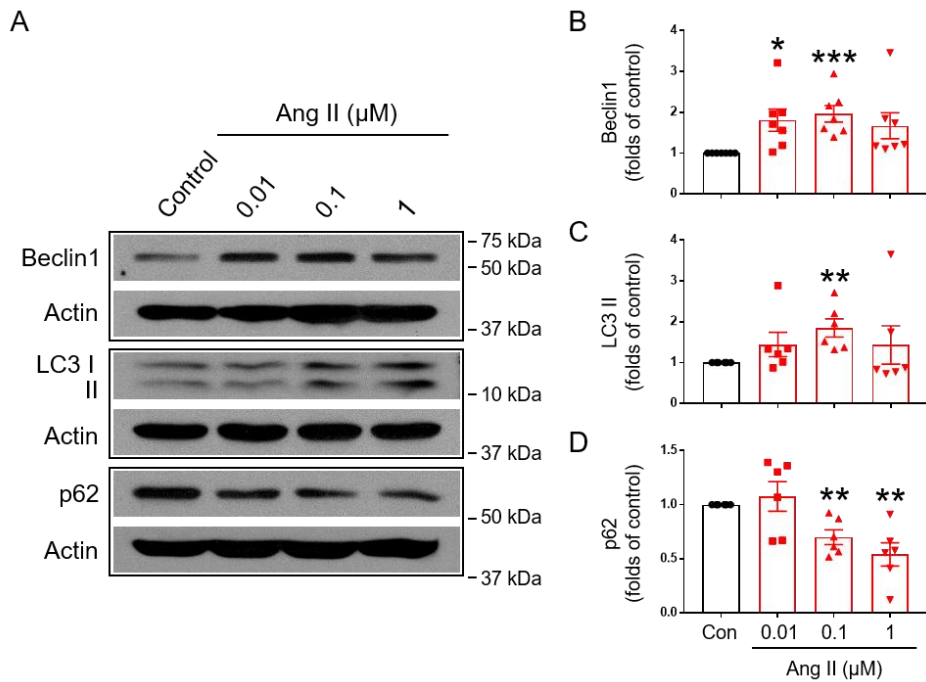


Figure 1. Effects of Ang II on the expression of autophagic markers in primary VSMCs. (A) Representative western blot analysis data for beclin1, LC3 A/B, and p62 expression in primary VSMCs. (B, C, and D) Quantitative data for beclin1 ($n = 7$), LC3 II ($n = 7$), and p62 ($n = 6$). Data are shown as means \pm SEM. * $p < 0.05$, ** $p < 0.01$, and *** $p < 0.001$ different from control. Con, control.

Effects of autophagy inhibitors on the expression of autophagic markers in VSMCs

To determine the effects of autophagy inhibitors on VSMCs, we used chloroquine and 3-methyladenine in VSMCs. The VSMCs were incubated with chloroquine (0, 10, 20, and 40 μ M) for 24 h (Fig. 2A₁). Chloroquine increased the expression of beclin1, LC3 II, and p62 in a dose-dependent manner. Chloroquine (20 μ M) was used for the following experiments. After co-treatment with Ang II (100 nM) and chloroquine, the expression of beclin1, LC3 II, and p62 increased (Fig. 2A₂).

VSMCs were incubated with 3-methyladenine (0, 1, 2.5, and 5 mM) for 24 h (Fig. 2B₁). We observed that 3-methyladenine decreased the expression of beclin1 and LC3 II in a dose-dependent manner, while p62 expression was increased in a dose-dependent manner. The 5 mM dose was used for subsequent experiments. After co-treatment with Ang II and 3-methyladenine, we examined the expression of the autophagy markers. We observed that 3-methyladenine reduced Ang II-induced increase in LC3 II and beclin1. A decrease in p62 expression induced by Ang II was reversed by 3-methyladenine (Fig. 2B₂). Acridine orange was used to stain acidic vesicular organelle, which reflect late-stage autophagy.³⁶ After 24 h starvation, VSMCs were incubated with Ang II, 3-methyladenine or Ang II + 3-methyladenine for 24 h. As shown in Figure 2C, Ang II enhanced late-stage autophagy, which was markedly reduced by 3-methyladenine.

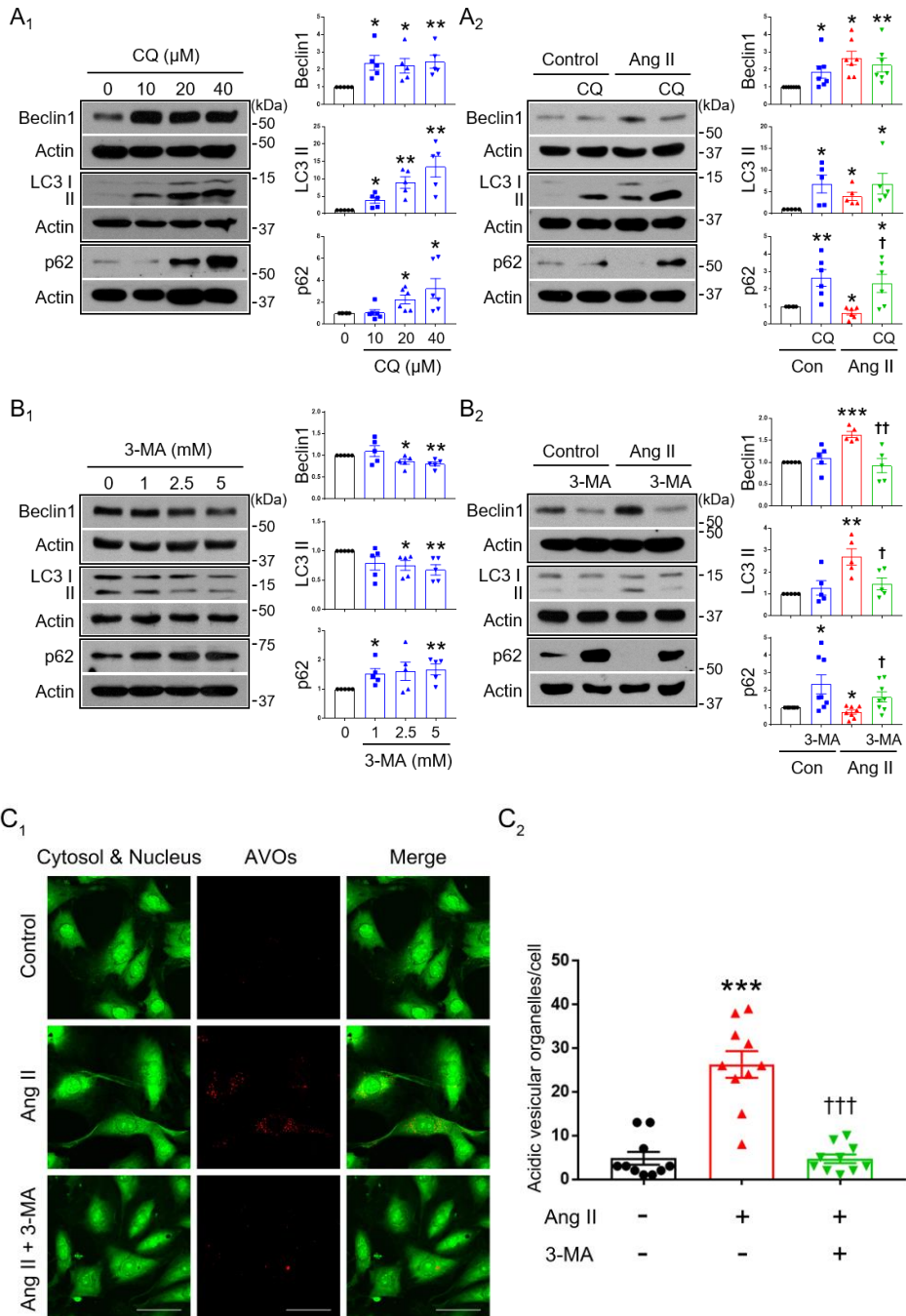


Figure 2. Effects of autophagy inhibitors on the expression of autophagic markers in primary VSMCs. (A₁) Western blot analysis data for beclin1, LC3 A/B, and p62 expression following treatment with various doses of chloroquine (CQ) (10 μ M, 20 μ M, and 40 μ M). n = 5 for beclin1 and LC3 A/B. n = 6 for p62. (A₂) Western blot analysis data for beclin1, LC3 A/B, and p62 expression following treatment with chloroquine (20 μ M), Ang II (100 nM) or co-treatment with Ang II and chloroquine for 24 h. n = 7 for beclin1. n = 5 for LC3 A/B. n = 6 for p62. (B₁) Western blot analysis data for beclin1, LC3 A/B, and p62 expression following treatment with various doses of 3-methyladenine (3-MA) (1 mM, 2.5 mM and 5 mM). n = 5 for each group. (B₂) Western blot analysis data for beclin1, LC3 A/B, and p62 expression following treatment with 3-methyladenine (5 mM) and, Ang II (100 nM) or co-treatment with Ang II and 3-methyladenine for 24 h. n = 5 for beclin1 and LC3 A/B. n = 8 for p62. (C₁) Representative images of acridine orange-stained primary VSMCs following treatment with Ang II or co-treatment with Ang II and 3-methyladenine for 24 h. (C₂) The graph represents the mean number of red puncta per cell. Scale bar = 50 μ m. The number of acidic vesicular organelles was counted from 10 randomly selected cells of 4 independent experiments and evaluated by ImageJ. Data are shown as means \pm SEM. *p < 0.05, **p < 0.01, and ***p < 0.001 different from the control, †p < 0.05, ††p < 0.01, †††p < 0.001 different from Ang II. AVOs, acidic vesicular organelles.

Effects of autophagy inhibitors on contractile responses in mesenteric arteries

To identify the role of autophagy in vasoconstriction induced by U46619 (100 nM), we used chloroquine and 3-methyladenine. Chloroquine and 3-methyladenine were used for treating mesenteric arteries pre-contracted with U46619 in a dose-dependent manner (Fig. 3). Chloroquine dose-dependently increased the diameter of the mesenteric arteries (Fig. 3A₁). The dose of 500 μ M that caused the maximal response ($61.0 \pm 2.3\%$) was used in the experiment shown in Figure 3A₃.

3-methyladenine dose-dependently increased the diameter of the mesenteric arteries (Fig. 3C₁). The relaxing effect of 3-methyladenine on vascular contractility in endothelium-denuded arteries was significantly reduced (Fig. 3C₂). The dose of 500 μ M that caused the maximal response ($84.9 \pm 3.5\%$) was used in the experiment shown in Figure 3C₃. These results show that direct administration of autophagy inhibitors induced vascular relaxation, which might be dependent on endothelial function.

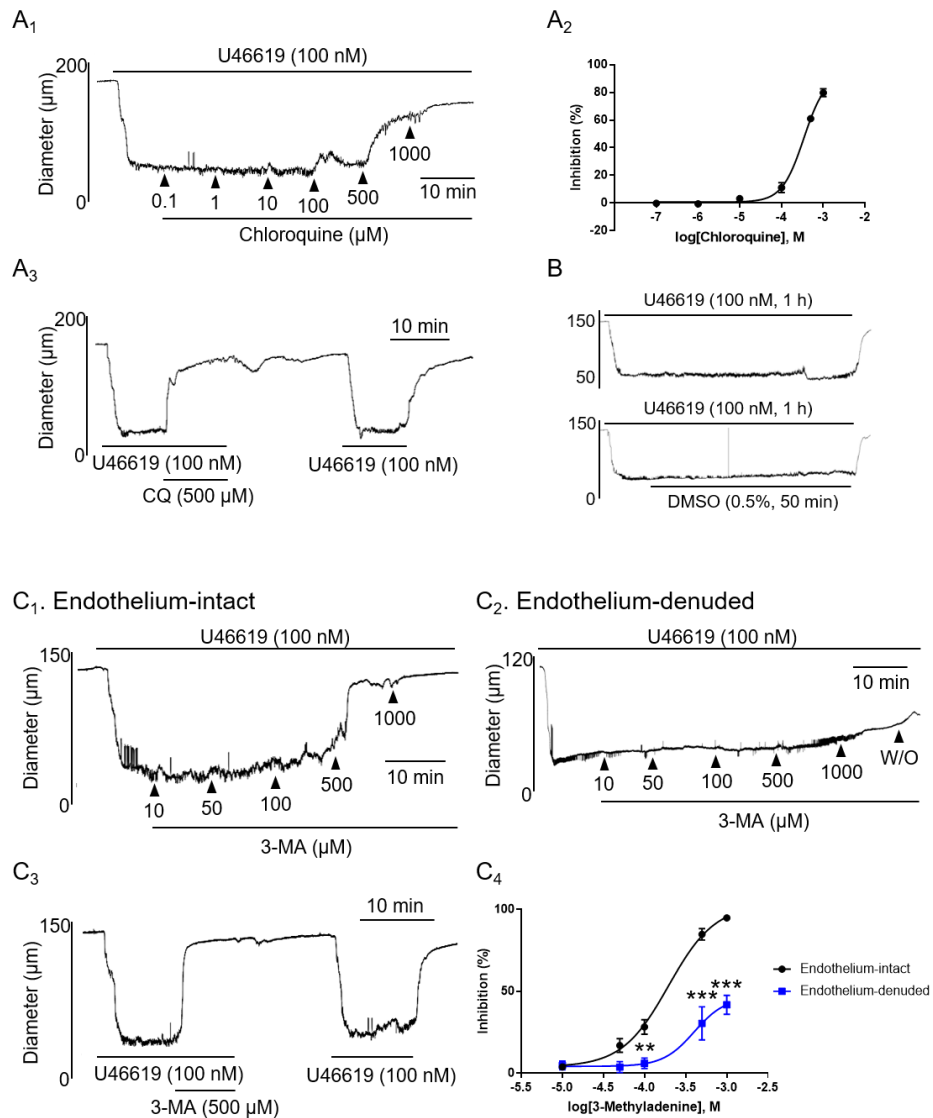


Figure 3. Dose-dependent response to chloroquine and 3-methyladenine in mesenteric arteries pre-contracted with U46619. (A₁ and A₃) Representative traces of the effect of chloroquine on the vasoconstriction induced by U46619. (A₂) Cumulative dose-response curve for chloroquine (n = 7). (B) U46619 (100 nM) time-control trace and DMSO-control trace (0.5%). (C₁ and C₃) Representative recordings of the effect of 3-methyladenine on the

vasocontraction induced by U46619 in endothelium-intact arteries. (C₂) Representative recordings of the effect of 3-methyladenine on the vasocontraction induced by U46619 in endothelium-denuded mesenteric arteries. (C₄) Cumulative dose-response curve for 3-methyladenine in intact (n = 6) or endothelium-denuded (n = 5) arteries. Data are shown as means \pm SEM. **p < 0.01, ***p < 0.001, for intact vs. endothelium-denuded arteries. W/O, wash out.

Effects of an autophagy inhibitor on blood pressure

To identify the physiological role of autophagy in blood pressure regulation, we measured systolic blood pressure in Ang II-induced hypertensive mice using the tail-cuff method as previously described.³⁹ The systolic blood pressure of Ang II-treated mice increased significantly compared with that of saline-treated mice. Injection of 3-methyladenine significantly reduced the blood pressure of Ang II-treated mice (vehicle, 114.8 ± 0.8 mmHg; vehicle + 3-methyladenine, 107.5 ± 5.0 mmHg; Ang II, 181.0 ± 6.2 mmHg; Ang II + 3-methyladenine, 134.4 ± 5.5 mmHg; at the end of experiments, Fig. 4A). There were no differences in body weight among groups (vehicle, 29.3 ± 0.8 g; vehicle + 3-methyladenine, 27.6 ± 0.8 g; Ang II, 27.0 ± 0.6 g; Ang II + 3-methyladenine, 26.2 ± 0.8 g; at the end of experiments, Fig. 4B). We analyzed the structure of the mesenteric arteries by measuring the lumen diameter and wall thickness. Ang II-treated mice had thicker mesenteric arteries, as evidenced by the increased wall/lumen ratio. Treatment with 3-methyladenine decreased the wall/lumen ratio of the mesenteric arteries compared with Ang II-treated mouse mesenteric arteries (Fig. 4C).

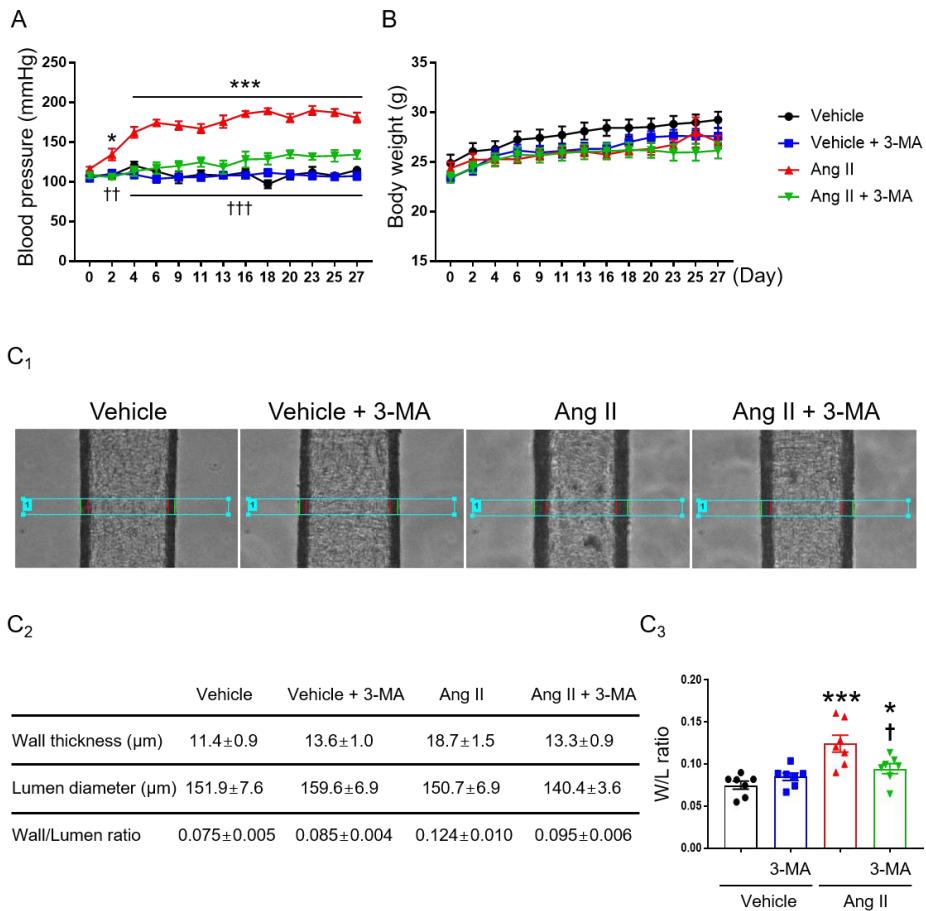
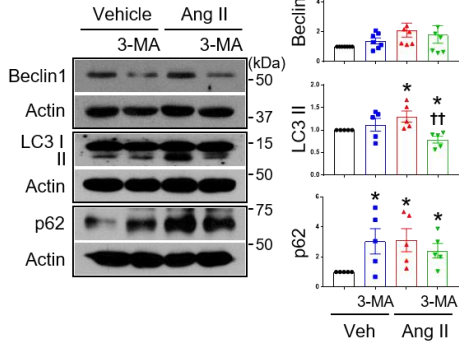


Figure 4. Effects of an autophagy inhibitor on blood pressure and body weight. Effects of an autophagy inhibitor on blood pressure and body weight. (A and B) Blood pressure and body weight in vehicle- and Ang II-treated (with or without 3-methyladenine) mice. (C₁) Representative images of the mesenteric arteries in resting state (40 mmHg). (C₂ and C₃) Wall/lumen ratio was measured from 7 randomly selected mouse mesenteric arteries for each independent groups. Data are shown as means \pm SEM. The n-values mean number animals. * $p < 0.05$, *** $p < 0.001$ for Vehicle vs. Ang II, † $p < 0.05$, †† $p < 0.01$, and ††† $p < 0.001$ for Ang II vs. Vehicle + Ang II. W/L ratio, wall thickness/lumen diameter ratio.

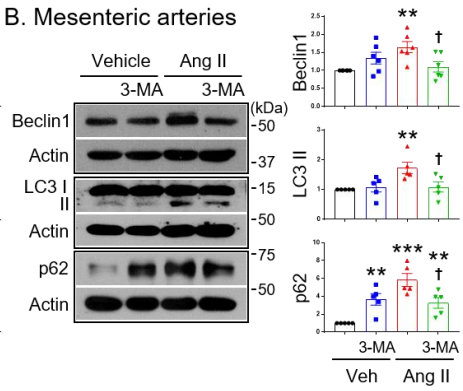
Effects of autophagy inhibitors on the expression of autophagic markers in the mesenteric arteries and aortas of Ang II-induced hypertensive mice

To investigate the *in vivo* role of autophagy in Ang II-induced hypertension, we performed western blot analysis with the mesenteric arteries and aortas of Ang II-treated mice. We found that the expression of beclin1, LC3 II, and p62 increased in Ang II-treated mice (Fig. 5A–B). To detect the increased expression of p62 in Ang II-treated mice, we examined the time-dependent effect of Ang II infusion on p62 levels. During the 1-week infusion, the level of p62 decreased in the aortas. However, chronic infusion of Ang II increased p62 levels (Fig. 5C). To strengthen the western blot analysis data, we measured the mRNA levels of p62 in the aortas of Ang II-treated mice. The gene expression of p62 was upregulated in mice infused with Ang II for 4 weeks compared with vehicle-treated mice (Fig. 5D). To support the western blot analysis data, we performed immunofluorescence staining analysis for beclin1 in the mesenteric arteries. Consistent with the western blotting results, the expression of beclin1 increased significantly in the mesenteric arteries of Ang II-treated mice, which was reduced by treatment with 3-methyladenine (Fig. 5E).

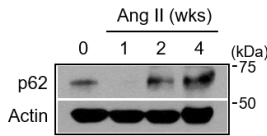
A. Aortas



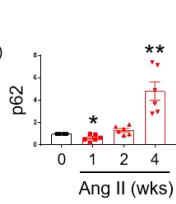
B. Mesenteric arteries



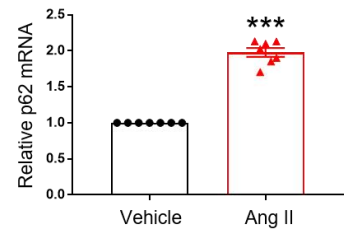
C₁



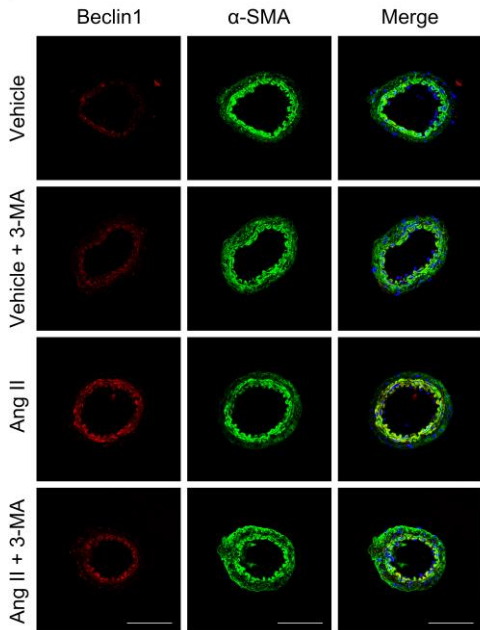
C₂



D



E₁



E₂

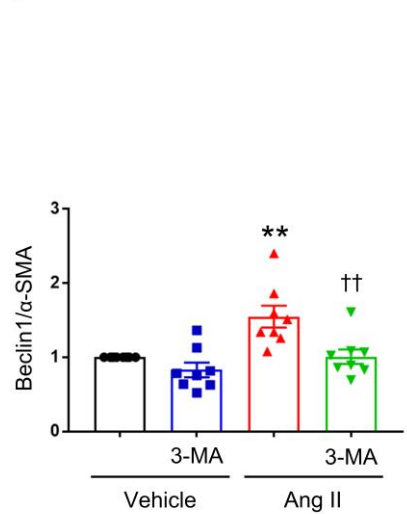


Figure 5. Effects of autophagy inhibitors on the expression of autophagic markers in the aortas and mesenteric arteries of Ang II-induced hypertensive mice. (A and B) Western blot analysis data for beclin1, LC3 A/B, and p62 in vehicle- and Ang II-treated (with or without 3-methyladenine) mouse aortas (n = 7 for beclin1, n = 5 for LC3 A/B and p62) and mesenteric arteries (n = 6 for beclin1, n = 5 for LC3 A/B and p62). (C₁) Western blot analysis data for p62 expression following treatment with Ang II for various time periods (1, 2, and 4 weeks). (C₂) Quantitative data for p62 (n = 6). (D) The graph represents the relative mRNA levels of p62 in the aortas following Ang II infusion (n = 7). (E₁) Representative immunofluorescence images of the mesenteric arteries following treatment with vehicle and Ang II (with or without 3-methyladenine). (E₂) The graph represents the mean data for beclin1 expression (n = 8). Scale bar = 100 μ m. Data are shown as means \pm SEM. The n-values mean number of animals. *p < 0.05, **p < 0.01, ***p < 0.001 different from vehicle, †p < 0.05, ††p < 0.01 different from Ang II. Veh, vehicle. α -SMA, α -smooth muscle actin.

Effects of autophagy inhibitors on endothelium-dependent relaxation in the mesenteric arteries of Ang II-induced hypertensive mice

We measured the endothelium-dependent relaxation of acetylcholine in the mesenteric arteries of Ang II-treated and vehicle-treated mice. Endothelium-dependent relaxation reduced significantly in Ang II-treated mice compared with vehicle-treated mice. The reduction of endothelium-dependent relaxation induced by Ang II was recovered by treatment with 3-methyladenine (Fig. 6A). Responses to sodium nitroprusside (nitric oxide donor) were not affected in any of the groups (Fig. 6B). Similarly, contraction responses to phenylephrine did not differ between groups (Fig. 6C).

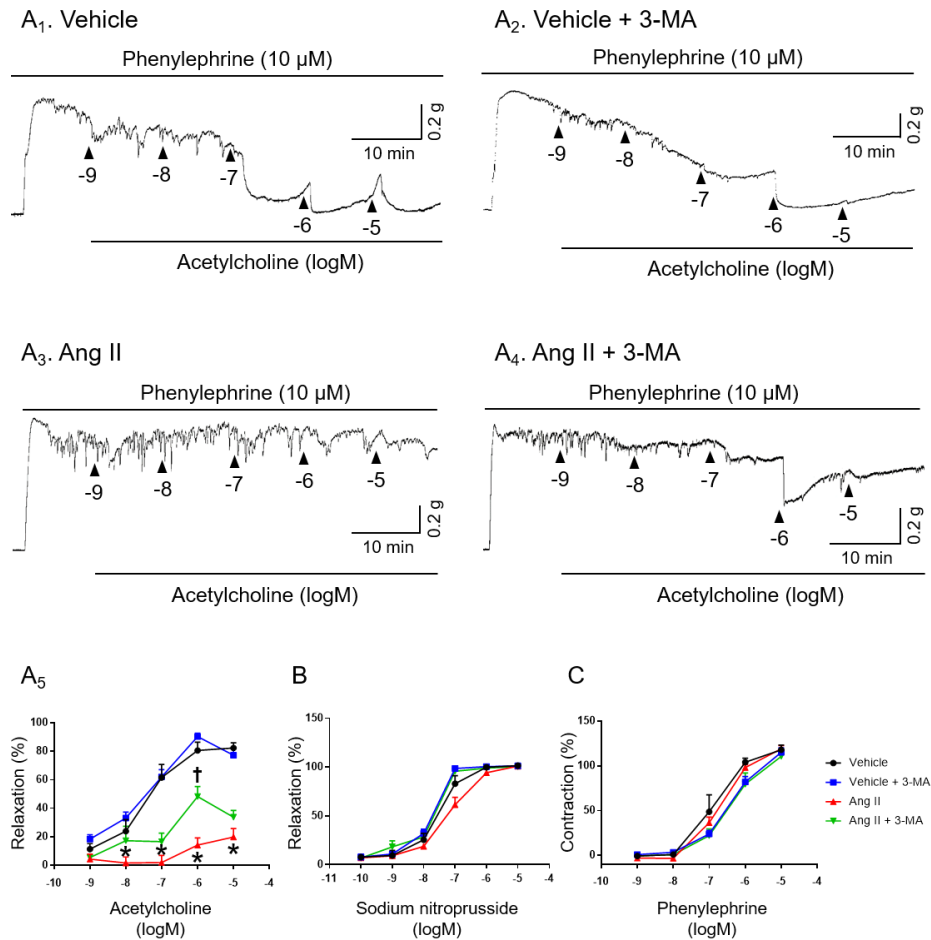


Figure 6. Effects of autophagy inhibitors on endothelium-dependent relaxation in the mesenteric arteries of Ang II-induced hypertensive mice.

(A₁₋₄) Representative recordings of endothelium-dependent relaxation in response to various doses (10^{-9} – 10^{-5} mol/L) on the vasoconstriction induced by phenylephrine (10 μM). (A₅) Mean data for endothelium-dependent relaxation (n = 11 for Vehicle and Vehicle + 3-MA, n = 8 for Ang II, n = 9 for Ang II + 3-MA). (B) Mean data for sodium nitroprusside-induced vasorelaxation (n = 6 for Vehicle and Ang II, n = 5 for Vehicle + 3-MA, n = 7 for Ang II + 3-MA). (C) Mean data for phenylephrine-induced vasoconstriction (n = 4 for Vehicle, n = 8 for Vehicle + 3-MA, Ang II, and Ang II + 3-MA). Data are shown as means ±

SEM. The n-values mean number of vessels derived from each different animals.

* $p < 0.05$ for Vehicle vs. Ang II, † $p < 0.05$ for Ang II vs. Vehicle + Ang II.

Autophagy inhibitor increases nitric oxide production in HUVECs and the mesenteric arteries

To measure nitric oxide levels in the mesenteric arteries, we used DAF-FM diacetate, a fluorescent indicator for nitric oxide. DAF-FM diacetate fluorescence intensity decreased in the mesenteric arteries from Ang II-treated mice compared with vehicle-treated or 3-methyladenine-treated mice. However, 3-methyladenine significantly restored DAF-FM diacetate fluorescence intensity in the mesenteric arteries of the Ang II-treated mice (Fig. 7A). In HUVECs, the levels of p-eNOS (S1177) were reduced by Ang II in a dose-dependent manner (10^{-8} – 10^{-6} mol/L, Fig 7B). We found that 3-methyladenine significantly rescued the levels of p-eNOS (S1177) in HUVECs (Fig. 7C). These data suggest that 3-methyladenine increases the production of nitric oxide in Ang II-induced hypertensive mice by regulating the levels of p-eNOS (S1177).

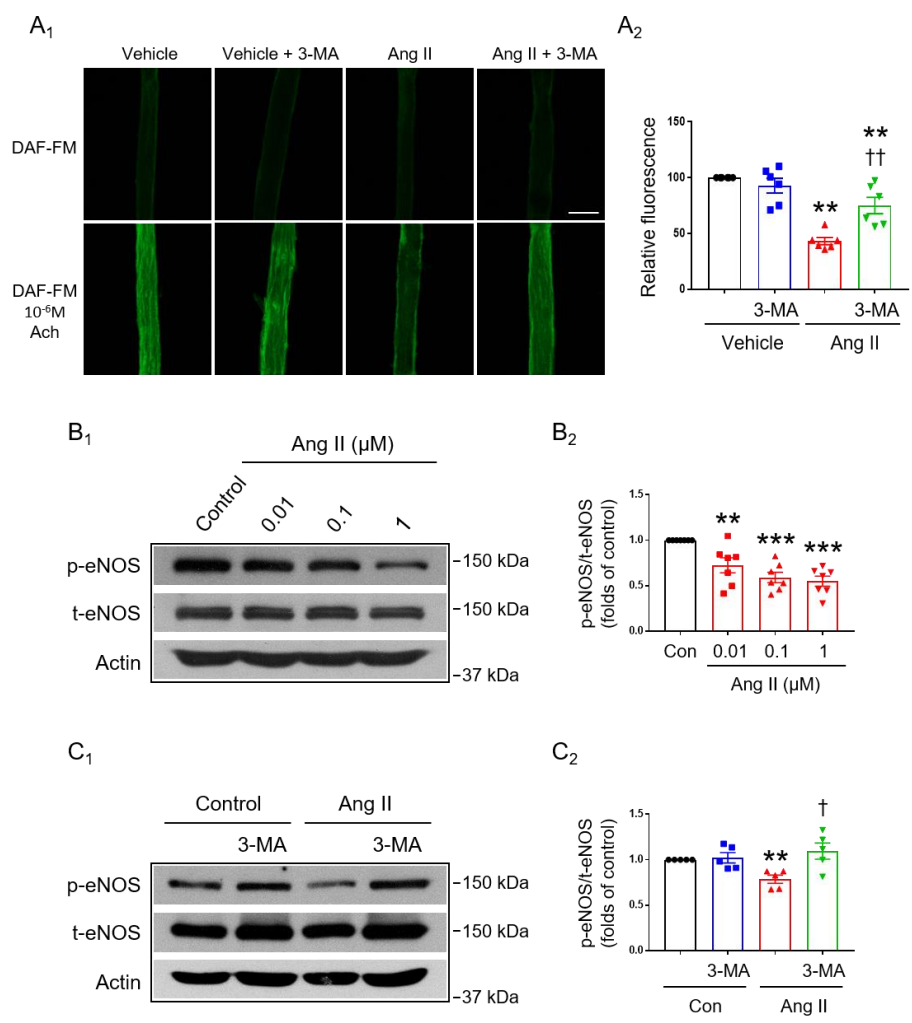


Figure 7. Effects of autophagy inhibitors on nitric oxide production in the mesenteric arteries and HUVECs. (A₁) Representative fluorescence images of mesenteric arteries incubated with DAF-FM diacetate (5 μM). The effect of acetylcholine (10⁻⁶ M) on mesenteric arteries incubated with DAF-FM diacetate in Vehicle, Vehicle + 3-MA, Ang II, and Ang II + 3-MA groups. Scale bar = 200 μm. (A₂) Mean data for the relative fluorescence intensity (n = 6). (B₁) Western blot analysis data for p-eNOS (S1177) and total-eNOS with Ang II (10⁻⁸–10⁻⁶ mol/L) for 24 h. (B₂) Mean data of p-eNOS and total-eNOS expression (n = 7). (C₁) Western blot analysis data for p-eNOS (S1177) and total-eNOS expression

following treatment with 3-methyladenine (5 mM) and, Ang II (100 nM) or co-treatment with Ang II and 3-methyladenine for 24 h. (C₂) Mean data of p-eNOS and total-eNOS expression (n = 5). Data are shown as means ± SEM. For nitric oxide detection, the n-values mean number of animals. **p < 0.01, ***p < 0.001 different from vehicle. †p < 0.05, ††p < 0.01 different from Ang II. Ach, acetylcholine.

IV. DISCUSSION

Autophagy is considered the new therapeutic target of various cardiovascular diseases such as pulmonary hypertension, atherosclerosis, and myocardial ischemia.^{20,21} However, the involvement of autophagy in the pathogenesis of hypertension remains unclear. In the present study, we found that the inhibition of excessive autophagy ameliorates endothelial dysfunction in Ang II-induced hypertension. Our results indicate that (i) Ang II increases autophagic flux, which is evidenced by the elevated levels of beclin1 and LC3 II, whereas Ang II decreases the level of p62; (ii) autophagy inhibitors have a relaxing effect on contractile responses in mesenteric arteries; (iii) in vivo treatment of an autophagy inhibitor decreases blood pressure and induces a reduction in wall/lumen ratio; and (iv) autophagy inhibitors improve endothelium-dependent relaxation by increasing nitric oxide production.

Ang II is the main component of the RAS,⁶ which increases blood pressure and vasoconstriction. Several in vitro studies have shown that Ang II induces autophagic flux in endothelial cells,³¹ vascular smooth muscle cells,^{32,33} cardiomyocytes,⁴⁰ and podocytes.^{30,41} In vivo studies have also shown that Ang II-infused mice exhibit enhanced autophagy.^{42,43} In accordance with previous studies, our results indicate that Ang II induces autophagy in VSMCs (Fig. 1).

Chloroquine is an approved drug used to prevent and treat malaria as well as inflammatory diseases.⁴⁴ Chloroquine is also known as an autophagy inhibitor and acts as a lysosomotropic agent that accumulates on lysosomes, where it is protonated. The protonated chloroquine alters the acidic environment of lysosomes, which blocks the late-stage of autophagy by inhibiting the binding of autophagosomes to lysosomes.^{45,46} A less toxic derivative of chloroquine, hydroxychloroquine was used in the present study.⁴⁷ In previous studies, chloroquine prevented lysosomal acidification, which led to the accumulation of beclin1, LC3 II, and p62 by blocking autophagy.⁴⁸⁻⁵⁰ However, there is a possibility that chloroquine induces lysosomal stress, which results in nucleus

translocation of transcription factor EB (TFEB) to initiate lysosomal biogenesis and autophagy.^{51,52} The TFEB serves as a master controller of lysosomal biogenesis by binding to the motif, i.e., the coordinated lysosomal expression and regulation element. The TFEB also binds to the promoter regions of the autophagy genes to induce autophagy.^{53,54} Although chloroquine can activate TFEB, it blocks autophagic flux effectively in VSMCs (Fig. 2A).

3-methyladenine is a well-known autophagy inhibitor that inhibits the formation of autophagosomes through the inhibitory effect of PI3K.⁵⁵ However, several concerns have been raised about the inhibitory effect of 3-methyladenine. 3-methyladenine can inhibit class I PI3K as well as class III PI3K.⁵⁶ In the PI3K/Akt/mammalian target of rapamycin (mTOR) signaling pathway, activation of class I PI3K consecutively activates mTOR, which negatively regulates autophagy induction. In contrast, autophagy is activated by class III PI3K, which is composed of the regulatory and catalytic subunits, Vps15 and Vps34, respectively.⁵⁷ The Vps34/Vps15/beclin1 complex controls autophagosome biogenesis and maturation.⁵⁸ The high concentration of 3-methyladenine can regulate other kinases and change other cellular metabolisms. For instance, glycogen breakdown through phosphofructokinase,⁵⁹ inhibition of the endocytosis pathway,⁶⁰ and mitochondrial permeability transition⁶¹ are regulated by high doses of 3-methyladenine (10–20 mM). The dose of 5 mM of 3-methyladenine, which is typically used, efficiently inhibits autophagic progress as demonstrated by various methods and assays *in vivo* and *in vitro*.⁶²⁻⁶⁴ In the present study, 5 mM of 3-methyladenine blocked the induction of autophagy in VSMCs (Fig. 2B–C). These data indicate that autophagy inhibitors induce changes of autophagic marker in VSMCs.

It has been shown that chloroquine has a relaxing effect on rat pulmonary arteries,⁶⁵ rat aorta,⁶⁶ and guinea pig trachea.⁶⁷ However, there is no evidence that autophagy contributes to the regulation of resistance in the mesenteric arteries. In the present study, we demonstrated that chloroquine and

3-methyladenine have vasodilatory effects on U46619-induced contraction in mesenteric arteries (Fig. 3). In a previous study, treatment with chloroquine led to vasodilation in endothelium-intact rat aorta, which was reduced by both the removal of endothelium and treatment with N ω -nitro-L-arginine methyl ester hydrochloride (an analog of arginine).⁶⁸ Similarly, our results showed that 3-methyladenine effectively decreased U46619-induced contraction in endothelium-intact mesenteric arteries, but not in endothelium-denuded mesenteric arteries. These data indicate that autophagy inhibitors induce vascular relaxation in mesenteric arteries of mice.

Several studies have reported that the dysregulation of autophagic flux is involved in various cardiovascular diseases, such as pulmonary hypertension,²² atherosclerosis,²⁴ and restenosis.⁶⁹ Augmented autophagy is responsible for establishing experimental pulmonary hypertension, which is inhibited by an autophagy inhibitor through its vasodilatory and antiproliferative effects.^{22,65} In spontaneously hypertensive rats, inhibition of autophagy or silencing LC3 II gene in the rostral ventrolateral medulla attenuates vasomotor tone and hypertension.³⁵ In the current study, intraperitoneal injection of 3-methyladenine significantly prevented the progression of hypertension, as evidenced by a decrease in blood pressure of Ang II-induced hypertensive mice (Fig. 4).

We observed autophagic marker levels in Ang II-induced hypertensive mice. As shown in Figure 5, the expression of beclin1, LC3 II, and p62 was increased by Ang II, which is inconsistent with our VSMC results. To identify the elevated levels of p62 in Ang II-treated mice, we measured the mRNA levels of p62 using quantitative RT-PCR. We found that chronic Ang II infusion induced p62 mRNA upregulation (Fig. 5E). Previous studies have shown that p62 is restored to basal levels during prolonged starvation, which depends on transcriptional upregulation.⁷⁰ The upregulation of p62 expression suggests adaptation to persistent starvation.

Elevated Ang II expression is a well-known contributor to endothelial

dysfunction in various vessels.⁷¹⁻⁷⁴ In the present study, Ang II-treated mice exhibited decreased endothelium-dependent relaxation, which was reversed by the injection of 3-methyladenine (Fig. 6). Based on these results, we hypothesized that 3-methyladenine had beneficial effects on vascular endothelial dysfunction. A similar study has reported that the inhibition of autophagy improves endothelial-dependent vasodilation of the coronary artery in animal models of myocardial infarction.⁷⁵ Previous studies have shown that Ang II-induced endothelial dysfunction is associated with defective nitric oxide production.^{73,76} It is widely known that Ang II regulates eNOS activity and expression.⁷⁷⁻⁷⁹ Therefore, we measured the phosphorylation levels of eNOS and nitric oxide production using DAF-FM diacetate (Fig. 7). Acetylcholine-induced nitric oxide production was decreased by treatment with Ang II, which was recovered by treatment with 3-methyladenine in mesenteric arteries (Fig. 7A). The level of p-eNOS (S1177) decreased by treatment of Ang II, which was restored by treatment of 3-methyladenine in HUVECs (Fig. 7C). These results suggest that autophagy inhibitors restore the activity of eNOS by phosphorylating eNOS (S1177).

Previous studies have suggested that the association of protein phosphatase 2A (PP2A, a ubiquitous serine/threonine phosphatase) and eNOS induces eNOS dephosphorylation (S1177).⁸⁰⁻⁸² A previous study has also shown that the activation of PP2A is required for autophagy induction. In the inactive state, PP2A interacts with its inhibitory protein, Alpha 4. Starvation induces the release of PP2A, resulting in the activation of PP2A and the induction of autophagy.⁸³ Although the signaling pathway between Ang II type 1 receptor and PP2A is not fully identified, we suggest that eNOS dephosphorylation is induced by PP2A, a phenomenon that is prevented by autophagy inhibition. Therefore, it seems that 3-methyladenine improves endothelium-dependent relaxation by regulating nitric oxide production in Ang II-induced hypertension. Our data suggest that chronic treatment with 3-methyladenine may be an

effective therapy for hypertension.

In summary, we suggest that excessive autophagy is involved in the progression of Ang II-induced hypertension. The inhibition of autophagy improves endothelial function by regulating eNOS phosphorylation both in vitro and in vivo. Our study demonstrates that the inhibition of excessive autophagy ameliorates vascular dysfunction in Ang II-induced hypertension.

V. CONCLUSION

In the present study, we discovered that (i) autophagy is increased in Ang II-induced hypertensive mice; (ii) chloroquine and 3-methyladenine effectively inhibit Ang II-induced autophagy in VSMCs; (iii) 3-methyladenine decreases elevated blood pressure induced by Ang II; and (iv) 3-methyladenine ameliorates endothelial dysfunction in Ang II-induced hypertensive mice by regulating nitric oxide production. Therefore, we suggest that the inhibition of excessive autophagy might improve endothelial dysfunction in hypertension induced by Ang II.

REFERENCES

1. Iulita MF, Vallerand D, Beauvillier M, Hauptert N, C AU, Gagne A, et al. Differential effect of angiotensin II and blood pressure on hippocampal inflammation in mice. *J Neuroinflammation* 2018;15:62.
2. de Lima RS, Silva JCS, Lima CT, de Souza LE, da Silva MB, Baladi MG, et al. Proinflammatory Role of Angiotensin II in the Aorta of Normotensive Mice. *Biomed Res Int* 2019;2019:9326896.
3. Choi SK, Lim M, Yeon SI, Lee YH. Inhibition of endoplasmic reticulum stress improves coronary artery function in type 2 diabetic mice. *Exp Physiol* 2016;101:768-77.
4. Brandes RP. Endothelial dysfunction and hypertension. *Hypertension* 2014;64:924-8.
5. Konukoglu D, Uzun H. Endothelial Dysfunction and Hypertension. *Adv Exp Med Biol* 2017;956:511-40.
6. Benigni A, Cassis P, Remuzzi G. Angiotensin II revisited: new roles in inflammation, immunology and aging. *EMBO Mol Med* 2010;2:247-57.
7. Reudelhuber TL. Where hypertension happens. *J Clin Invest* 2013;123:1934-6.
8. Crowley SD, Gurley SB, Herrera MJ, Ruiz P, Griffiths R, Kumar AP, et al. Angiotensin II causes hypertension and cardiac hypertrophy through its receptors in the kidney. *Proc Natl Acad Sci U S A* 2006;103:17985-90.
9. Nguyen Dinh Cat A, Montezano AC, Burger D, Touyz RM. Angiotensin II, NADPH oxidase, and redox signaling in the vasculature. *Antioxid Redox Signal* 2013;19:1110-20.
10. Ruster C, Wolf G. Renin-angiotensin-aldosterone system and progression of renal disease. *J Am Soc Nephrol* 2006;17:2985-91.
11. Levine B, Kroemer G. Autophagy in the pathogenesis of disease. *Cell* 2008;132:27-42.
12. Glick D, Barth S, Macleod KF. Autophagy: cellular and molecular mechanisms. *J Pathol* 2010;221:3-12.
13. Mizushima N, Komatsu M. Autophagy: renovation of cells and tissues. *Cell* 2011;147:728-41.
14. Li X, He S, Ma B. Autophagy and autophagy-related proteins in cancer. *Mol Cancer* 2020;19:12.
15. Hill SM, Wrobel L, Rubinsztein DC. Post-translational modifications of Beclin 1 provide multiple strategies for autophagy regulation. *Cell Death Differ* 2019;26:617-29.
16. Xie Y, Kang R, Sun X, Zhong M, Huang J, Klionsky DJ, et al. Posttranslational modification of autophagy-related proteins in macroautophagy. *Autophagy* 2015;11:28-45.
17. Mei Y, Thompson MD, Cohen RA, Tong X. Autophagy and oxidative stress in cardiovascular diseases. *Biochim Biophys Acta* 2015;1852:243-51.
18. Liu WJ, Ye L, Huang WF, Guo LJ, Xu ZG, Wu HL, et al. p62 links the autophagy pathway and the ubiquitin-proteasome system upon ubiquitinated protein degradation. *Cell Mol Biol Lett* 2016;21:29.
19. Ravanan P, Srikumar IF, Talwar P. Autophagy: The spotlight for cellular stress responses. *Life Sci* 2017;188:53-67.

20. Wang ZV, Rothermel BA, Hill JA. Autophagy in hypertensive heart disease. *J Biol Chem* 2010;285:8509-14.
21. Tai S, Hu XQ, Peng DQ, Zhou SH, Zheng XL. The roles of autophagy in vascular smooth muscle cells. *Int J Cardiol* 2016;211:1-6.
22. Long L, Yang X, Southwood M, Lu J, Marciniak SJ, Dunmore BJ, et al. Chloroquine prevents progression of experimental pulmonary hypertension via inhibition of autophagy and lysosomal bone morphogenetic protein type II receptor degradation. *Circ Res* 2013;112:1159-70.
23. Lee SJ, Smith A, Guo L, Alastalo TP, Li M, Sawada H, et al. Autophagic protein LC3B confers resistance against hypoxia-induced pulmonary hypertension. *Am J Respir Crit Care Med* 2011;183:649-58.
24. Martinet W, De Meyer GR. Autophagy in atherosclerosis: a cell survival and death phenomenon with therapeutic potential. *Circ Res* 2009;104:304-17.
25. Chen R, Jiang M, Li B, Zhong W, Wang Z, Yuan W, et al. The role of autophagy in pulmonary hypertension: a double-edge sword. *Apoptosis* 2018;23:459-69.
26. Osonoi Y, Mita T, Azuma K, Nakajima K, Masuyama A, Goto H, et al. Defective autophagy in vascular smooth muscle cells enhances cell death and atherosclerosis. *Autophagy* 2018;14:1991-2006.
27. Perrotta I. Occurrence and characterization of lipofuscin and ceroid in human atherosclerotic plaque. *Ultrastruct Pathol* 2018;42:477-88.
28. Porrello ER, D'Amore A, Curl CL, Allen AM, Harrap SB, Thomas WG, et al. Angiotensin II type 2 receptor antagonizes angiotensin II type 1 receptor-mediated cardiomyocyte autophagy. *Hypertension* 2009;53:1032-40.
29. Liu S, Chen S, Li M, Zhang B, Shen P, Liu P, et al. Autophagy activation attenuates angiotensin II-induced cardiac fibrosis. *Arch Biochem Biophys* 2016;590:37-47.
30. Yadav A, Vallabu S, Arora S, Tandon P, Slahan D, Teichberg S, et al. ANG II promotes autophagy in podocytes. *Am J Physiol Cell Physiol* 2010;299:C488-96.
31. Chen F, Chen B, Xiao FQ, Wu YT, Wang RH, Sun ZW, et al. Autophagy protects against senescence and apoptosis via the RAS-mitochondria in high-glucose-induced endothelial cells. *Cell Physiol Biochem* 2014;33:1058-74.
32. Yu KY, Wang YP, Wang LH, Jian Y, Zhao XD, Chen JW, et al. Mitochondrial KATP channel involvement in angiotensin II-induced autophagy in vascular smooth muscle cells. *Basic Res Cardiol* 2014;109:416.
33. Mondaca-Ruff D, Riquelme JA, Quiroga C, Norambuena-Soto I, Sanhueza-Olivares F, Villar-Fincheira P, et al. Angiotensin II-Regulated Autophagy Is Required for Vascular Smooth Muscle Cell Hypertrophy. *Front Pharmacol* 2018;9:1553.
34. Zhou L, Ma B, Han X. The role of autophagy in angiotensin II-induced pathological cardiac hypertrophy. *J Mol Endocrinol* 2016;57:R143-R52.
35. Chao YM, Lai MD, Chan JY. Redox-sensitive endoplasmic reticulum stress and autophagy at rostral ventrolateral medulla contribute to hypertension in spontaneously hypertensive rats. *Hypertension* 2013;61:1270-80.
36. SenthilKumar G, Skiba JH, Kimple RJ. High-throughput quantitative detection of basal autophagy and autophagic flux using image cytometry. *Biotechniques*

- 2019;67:70-3.
37. Thome MP, Filippi-Chiela EC, Villodre ES, Migliavaca CB, Onzi GR, Felipe KB, et al. Ratiometric analysis of Acridine Orange staining in the study of acidic organelles and autophagy. *J Cell Sci* 2016;129:4622-32.
 38. Yeon SI, Kim JY, Yeon DS, Abramowitz J, Birnbaumer L, Muallem S, et al. Transient receptor potential canonical type 3 channels control the vascular contractility of mouse mesenteric arteries. *PLoS One* 2014;9:e110413.
 39. Choi SK, Lim M, Byeon SH, Lee YH. Inhibition of endoplasmic reticulum stress improves coronary artery function in the spontaneously hypertensive rats. *Sci Rep* 2016;6:31925.
 40. Lin L, Liu X, Xu J, Weng L, Ren J, Ge J, et al. Mas receptor mediates cardioprotection of angiotensin-(1-7) against Angiotensin II-induced cardiomyocyte autophagy and cardiac remodeling through inhibition of oxidative stress. *J Cell Mol Med* 2016;20:48-57.
 41. Mao N, Tan RZ, Wang SQ, Wei C, Shi XL, Fan JM, et al. Ginsenoside Rg1 inhibits angiotensin II-induced podocyte autophagy via AMPK/mTOR/PI3K pathway. *Cell Biol Int* 2016;40:917-25.
 42. Shen Q, Bi X, Ling L, Ding W. 1,25-Dihydroxyvitamin D3 Attenuates Angiotensin II-Induced Renal Injury by Inhibiting Mitochondrial Dysfunction and Autophagy. *Cell Physiol Biochem* 2018;51:1751-62.
 43. Cheng Z, Zhang M, Hu J, Lin J, Feng X, Wang S, et al. Mst1 knockout enhances cardiomyocyte autophagic flux to alleviate angiotensin II-induced cardiac injury independent of angiotensin II receptors. *J Mol Cell Cardiol* 2018;125:117-28.
 44. Mauthe M, Orhon I, Rocchi C, Zhou X, Luhr M, Hijlkema KJ, et al. Chloroquine inhibits autophagic flux by decreasing autophagosome-lysosome fusion. *Autophagy* 2018;14:1435-55.
 45. Redmann M, Benavides GA, Berryhill TF, Wani WY, Ouyang XS, Johnson MS, et al. Inhibition of autophagy with bafilomycin and chloroquine decreases mitochondrial quality and bioenergetic function in primary neurons. *Redox Biology* 2017;11:73-81.
 46. Jia BX, Xue YN, Yan XY, Li JL, Wu Y, Guo R, et al. Autophagy inhibitor chloroquine induces apoptosis of cholangiocarcinoma cells via endoplasmic reticulum stress. *Oncology Letters* 2018;16:3509-16.
 47. Liu J, Cao R, Xu M, Wang X, Zhang H, Hu H, et al. Hydroxychloroquine, a less toxic derivative of chloroquine, is effective in inhibiting SARS-CoV-2 infection in vitro. *Cell Discov* 2020;6:16.
 48. Yuan X, Xiao YC, Zhang GP, Hou N, Wu XQ, Chen WL, et al. Chloroquine improves left ventricle diastolic function in streptozotocin-induced diabetic mice. *Drug Design Development and Therapy* 2016;10:2729-37.
 49. Moon JH, Eo SK, Lee JH, Park SY. Quercetin-induced autophagy flux enhances TRAIL-mediated tumor cell death. *Oncology Reports* 2015;34:375-81.
 50. Wang X, Sun D, Hu Y, Xu X, Jiang W, Shang H, et al. The roles of oxidative stress and Beclin-1 in the autophagosome clearance impairment triggered by cardiac arrest. *Free Radic Biol Med* 2019;136:87-95.
 51. Zhitomirsky B, Yunaev A, Kreiserman R, Kaplan A, Stark M, Assaraf YG. Lysosomotropic drugs activate TFEB via lysosomal membrane fluidization and

- consequent inhibition of mTORC1 activity. *Cell Death Dis* 2018;9:1191.
52. Lu S, Sung T, Lin N, Abraham RT, Jessen BA. Lysosomal adaptation: How cells respond to lysosomotropic compounds. *PLoS One* 2017;12:e0173771.
 53. Settembre C, Di Malta C, Polito VA, Garcia Arencibia M, Vetrini F, Erdin S, et al. TFEB links autophagy to lysosomal biogenesis. *Science* 2011;332:1429-33.
 54. Napolitano G, Ballabio A. TFEB at a glance. *J Cell Sci* 2016;129:2475-81.
 55. Dai S, Wang B, Li W, Wang L, Song X, Guo C, et al. Systemic application of 3-methyladenine markedly inhibited atherosclerotic lesion in ApoE(-/-) mice by modulating autophagy, foam cell formation and immune-negative molecules. *Cell Death Dis* 2016;7:e2498.
 56. Wu YT, Tan HL, Shui G, Bauvy C, Huang Q, Wenk MR, et al. Dual role of 3-methyladenine in modulation of autophagy via different temporal patterns of inhibition on class I and III phosphoinositide 3-kinase. *J Biol Chem* 2010;285:10850-61.
 57. Nemazanyy I, Montagnac G, Russell RC, Morzyglod L, Burnol AF, Guan KL, et al. Class III PI3K regulates organismal glucose homeostasis by providing negative feedback on hepatic insulin signalling. *Nat Commun* 2015;6:8283.
 58. Morris DH, Yip CK, Shi Y, Chait BT, Wang QJ. Beclin 1-Vps34 Complex Architecture: Understanding the Nuts and Bolts of Therapeutic Targets. *Front Biol (Beijing)* 2015;10:398-426.
 59. Caro LH, Plomp PJ, Wolvetang EJ, Kerkhof C, Meijer AJ. 3-Methyladenine, an inhibitor of autophagy, has multiple effects on metabolism. *Eur J Biochem* 1988;175:325-9.
 60. Punnonen EL, Marjomaki VS, Reunanen H. 3-Methyladenine inhibits transport from late endosomes to lysosomes in cultured rat and mouse fibroblasts. *Eur J Cell Biol* 1994;65:14-25.
 61. Xue L, Borutaite V, Tolkovsky AM. Inhibition of mitochondrial permeability transition and release of cytochrome c by anti-apoptotic nucleoside analogues. *Biochem Pharmacol* 2002;64:441-9.
 62. Liu Y, Li D, He Z, Liu Q, Wu J, Guan X, et al. Inhibition of autophagy-attenuated calcium oxalate crystal-induced renal tubular epithelial cell injury in vivo and in vitro. *Oncotarget* 2018;9:4571-82.
 63. Wang JY, Xia Q, Chu KT, Pan J, Sun LN, Zeng B, et al. Severe global cerebral ischemia-induced programmed necrosis of hippocampal CA1 neurons in rat is prevented by 3-methyladenine: a widely used inhibitor of autophagy. *J Neuropathol Exp Neurol* 2011;70:314-22.
 64. Zhang Y, Liu G, Dull RO, Schwartz DE, Hu G. Autophagy in pulmonary macrophages mediates lung inflammatory injury via NLRP3 inflammasome activation during mechanical ventilation. *Am J Physiol Lung Cell Mol Physiol* 2014;307:L173-85.
 65. Wu K, Zhang Q, Wu X, Lu W, Tang H, Liang Z, et al. Chloroquine is a potent pulmonary vasodilator that attenuates hypoxia-induced pulmonary hypertension. *Br J Pharmacol* 2017;174:4155-72.
 66. Aziba PI, Okpako DT. Effects of chloroquine on smooth muscle contracted with noradrenaline or high-potassium solutions in the rat thoracic aorta. *J Smooth Muscle Res* 2003;39:31-7.
 67. Pulkkinen V, Manson ML, Saffholm J, Adner M, Dahlen SE. The bitter taste receptor (TAS2R) agonists denatonium and chloroquine display distinct

- patterns of relaxation of the guinea pig trachea. *Am J Physiol Lung Cell Mol Physiol* 2012;303:L956-66.
68. Pestana CR, Oishi JC, Salistre-Araujo HS, Rodrigues GJ. Inhibition of autophagy by chloroquine stimulates nitric oxide production and protects endothelial function during serum deprivation. *Cell Physiol Biochem* 2015;37:1168-77.
 69. Grootaert MO, da Costa Martins PA, Bitsch N, Pintelon I, De Meyer GR, Martinet W, et al. Defective autophagy in vascular smooth muscle cells accelerates senescence and promotes neointima formation and atherogenesis. *Autophagy* 2015;11:2014-32.
 70. Sahani MH, Itakura E, Mizushima N. Expression of the autophagy substrate SQSTM1/p62 is restored during prolonged starvation depending on transcriptional upregulation and autophagy-derived amino acids. *Autophagy* 2014;10:431-41.
 71. Gomolak JR, Didion SP. Angiotensin II-induced endothelial dysfunction is temporally linked with increases in interleukin-6 and vascular macrophage accumulation. *Front Physiol* 2014;5:396.
 72. Watanabe T, Barker TA, Berk BC. Angiotensin II and the endothelium: diverse signals and effects. *Hypertension* 2005;45:163-9.
 73. Shatanawi A, Romero MJ, Iddings JA, Chandra S, Umapathy NS, Verin AD, et al. Angiotensin II-induced vascular endothelial dysfunction through RhoA/Rho kinase/p38 mitogen-activated protein kinase/arginase pathway. *Am J Physiol Cell Physiol* 2011;300:C1181-92.
 74. van der Graaf AM, Wiegman MJ, Plosch T, Zeeman GG, van Buiten A, Henning RH, et al. Endothelium-dependent relaxation and angiotensin II sensitivity in experimental preeclampsia. *PLoS One* 2013;8:e79884.
 75. Wang R, Yang Q, Wang X, Wang W, Li J, Zhu J, et al. FoxO3 α -mediated autophagy contributes to apoptosis in cardiac microvascular endothelial cells under hypoxia. *Microvasc Res* 2016;104:23-31.
 76. Satoh M, Fujimoto S, Arakawa S, Yada T, Namikoshi T, Haruna Y, et al. Angiotensin II type 1 receptor blocker ameliorates uncoupled endothelial nitric oxide synthase in rats with experimental diabetic nephropathy. *Nephrol Dial Transplant* 2008;23:3806-13.
 77. Mehta PK, Griendling KK. Angiotensin II cell signaling: physiological and pathological effects in the cardiovascular system. *Am J Physiol Cell Physiol* 2007;292:C82-97.
 78. Raij L. The pathophysiologic basis for blocking the renin-angiotensin system in hypertensive patients with renal disease. *Am J Hypertens* 2005;18:95S-9S.
 79. Ratliff BB, Sekulic M, Rodebaugh J, Solhaug MJ. Angiotensin II regulates NOS expression in afferent arterioles of the developing porcine kidney. *Pediatr Res* 2010;68:29-34.
 80. Wei Q, Xia Y. Proteasome inhibition down-regulates endothelial nitric-oxide synthase phosphorylation and function. *Journal of Biological Chemistry* 2006;281:21652-9.
 81. Greif DM, Kou RQ, Michel T. Site-specific dephosphorylation of endothelial nitric oxide synthase by protein phosphatase 2A: Evidence for crosstalk between phosphorylation sites. *Biochemistry* 2002;41:15845-53.
 82. Li J, Geng XY, Cong XL. PGC-1 α ameliorates AngiotensinII-induced

- eNOS dysfunction in human aortic endothelial cells. *Vascular Pharmacology* 2016;83:90-7.
83. Wong PM, Feng Y, Wang JR, Shi R, Jiang XJ. Regulation of autophagy by coordinated action of mTORC1 and protein phosphatase 2A. *Nature Communications* 2015;6.

ABSTRACT(IN KOREAN)

Angiotensin II로 유도된 고혈압 동물에서 자가포식 억제를 통한
말초혈관 기능이상 개선

< 지도교수 이 영 호 >

연세대학교 대학원 의과학과

권 영 인

자가포식(autophagy)은 자가포식소체(autophagosome)와 리소좀(lysosome)을 통해 세포질의 노폐물, 퇴행성 단백질, 기능을 하지 못하는 세포소기관을 분해하는 세포 내 분해 시스템이다. 최근 많은 연구에서 폐동맥 고혈압, 죽상동맥경화증, 심근허혈 등 심혈관 질환과 자가포식의 연관성이 보고되었으나 고혈압과 자가포식의 연관성은 아직 명확히 밝혀지지 않았다. 따라서 본 연구에서는 자가포식이 안지오텐신 II(angiotensin II)로 유도된 고혈압 마우스의 혈압 변화와 장간막 동맥(mesenteric artery)의 기능 장애에 관련하는지 규명하고자 하였다.

안지오텐신 II는 자가포식 관련 단백질(Atg protein, autophagy-related protein)인 beclin1과 LC3 II의 발현을 증가시키고 p62의 발현을 감소를 유발했지만 자가포식 억제제인 클로로퀸(chloroquine)은 beclin1, LC3 II, p62 모두를 증가시켰다. 또 다른 자가포식 억제제인 3-메틸아데닌(3-methyladenine) 역시 안지오텐신 II에 의해 증가된 beclin1과 LC3 II를 유의하게

감소시키고 안지오텐신 II에 의해 감소된 p62를 증가시켰다. 즉 안지오텐신 II에 의해 증가된 자가포식을 클로로퀸과 3-메틸아데닌이 억제함을 확인하였다. 장간막 동맥에서 U46619에 의해 유도된 수축을 클로로퀸과 3-메틸아데닌이 농도 의존적으로 이완시켰다. 안지오텐신 II로 유도된 고혈압 마우스에서 자가포식의 역할을 알아보기 위해 고혈압 마우스에 3-메틸아데닌(30mg/kg)을 4주 동안 1일 1회씩 복강 내 주사하였다. 3-메틸아데닌 약물 주입은 고혈압 마우스의 혈압을 유의하게 강하시켰다. 고혈압에서 보이는 혈관 기능 이상에 자가포식이 관여하는지 확인하기 위해 내피세포 의존성 혈관 이완(endothelium-dependent relaxation)을 확인하였다. 고혈압 마우스에서 감소되어 있는 내피세포 의존성 혈관 이완이 3-메틸아데닌 약물 주입에 의해 개선됨을 확인하였고 나이트로프루사이드 나트륨(sodium nitroprusside)에 의한 이완은 차이가 없음을 확인하였다. 페닐에프린(phenylephrine)에 의한 수축은 차이가 없음을 확인하였다. 산화질소(nitric oxide)의 지표인 DAF-FM 디아세테이트(diacetate)의 형광 강도를 측정하여 산화질소의 검출을 확인하였다. 고혈압 마우스에서 감소되어 있는 DAF-FM 디아세테이트 형광 강도가 3-메틸아데닌 약물 주입에 의해 개선됨을 확인하였다. 안지오텐신 II 처리에 의해 내피 산화질소 신타아제(endothelial nitric oxide synthase)의 인산화가 감소되었고 3-메틸아데닌 처리에 의해 증가됨을 확인하였다.

결론적으로, 자가포식 억제는 안지오텐신 II로 유도된 고혈압 마우스의 혈압상승을 억제하고, 이는 내피세포 의존성 혈관 이완의 개선과 관련이 있음을 밝혔다. 따라서 본 연구에서는 자가포식 억제를 고혈압에서 나타나는 동맥 기능 부전을 개선시킬 수 있는 새로운 치료 표적으로 제시한다.

핵심되는 말 : 자가포식, 고혈압, 안지오텐신 II, 장간막 동맥, 내피 의존성 이완

PUBLICATION LIST

1. **Kwon Y**, Haam CE, Byeon S, Choi SJ, Shin DH, Choi SK, et al. Vasodilatory effect of Phellinus linteus extract in rat mesenteric arteries. *Molecules* 2020;25:3160.
2. Choi SK, **Kwon Y**, Byeon S, Haam CE, Lee YH. AdipoRon, adiponectin receptor agonist, improves vascular function in the mesenteric arteries of type 2 diabetic mice. *PLoS One* 2020;15:e0230227.
3. Choi SK, **Kwon Y**, Byeon S, Lee YH. Stimulation of autophagy improves vascular function in the mesenteric arteries of type 2 diabetic mice. *Exp Physiol* 2020;105:192-200.
4. **Kwon Y**, Choi SK, Byeon S, Lee YH. Involvement of inhibitor kappa B kinase 2 (IKK2) in the regulation of vascular tone. *Lab Invest* 2018;10:1311-1319.
5. Choi SK, Yeon SI, **Kwon Y**, Byeon S, Lee YH. Involvement of epithelial Na²⁺ channel in the elevated myogenic response in posterior cerebral arteries from spontaneously hypertensive rats. *Sci Rep* 2017;7:45996.